We are grateful to the referees for their time and energy in providing helpful comments and guidance that have improved the manuscript. In this document, we describe how we have addressed the reviewer's comments. Referee comments are shown in black italics and author responses are shown in blue regular text.

Referee 1

This vegetation model-based quantification of various components, including rising CO2, O3 pollution, and warming, influencing carbon sequestration across terrestrial ecosystems in China is not less than being complete. Moreover, there are many places that are quite interesting to me and would appeal to the broad communities around ACP. For example, to supplement with diffuse radiation the CMIP5 data the authors compiled empirical relationships between total and diffuse radiation and identified the best one therein to derive the diffuse radiation. What's also interesting is that the authors drew a conclusion that the allowable carbon budget is higher than expected to achieve the 1.5 deg C goal under a stabilized pathway.

➔ Thank you for your positive evaluations.

However, one major concern among other smaller ones is about land use change, which throughout the simulations with two different pathways the land cover is assumed fixed. The impacts of land cover change on the land carbon sink are undoubtedly tremendous. I argue it is more persuasive to include this in the quantification, especially considering the effort by the authors trying to offer numbers on allowable carbon budget.

➔ We agree that land cover change (LCC) can induce different responses in regional carbon budget for different emission pathways. However, "For this study, we fix the land cover to isolate impacts of CO_2 and climatic changes." The effect of LCC can be quantitatively evaluated using TRENDY data shown as below:

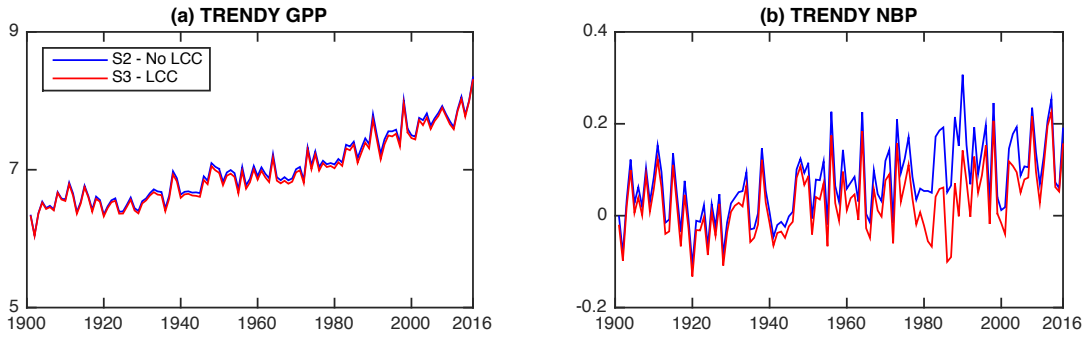

Fig. R1 Multi-model ensemble mean (a) GPP and (b) NBP from TRENDY for S2 (fixed land cover, blue) and S3 (with LCC, red) simulations. Units: Pg C yr^{-1}.

In the above figure, we compare multi-model ensemble mean GPP and NBP with and without LCC in China. As it shows, the differences are only 0.6±0.2% for GPP

between simulations with (S3) and without (S2) LCC during 1901-2016 (Fig. R1a). The TRENDY dataset does not provide NEE for all models. Instead, it has net biospheric production (NBP = – NEE – LCC). For NBP, we can see some differences between the two simulations (Fig. R1b), especially over the 1980s when S3 is less positive than that of S2. This change means that land carbon sink is weakened (or more land carbon emissions) due to LCC in the 1980s. However, this change is not caused through the perturbations in ecosystem but by anthropogenic activities, because GPP with LCC shows little changes (Fig. R1a). From this aspect, the LCC acts as an additional anthropogenic emission, instead of ecosystem responses.

Furthermore, the LCC changes in China are very uncertain (or unrealistic). From TRENDY simulations, we can see that NBP is lower in S3 than S2 during 2000-2016, indicating that LCC weakens land carbon sink. However, satellite observations suggest that afforestation significantly contributes to the greening in China over the recent decades (Chen et al., 2019), indicating that LCC actually strengthens regional carbon sink. For the future projections, LCC is even more uncertain because it is related to many policy-related and economic factors (Stehfest et al., 2019) that are not associated with CO_2 emissions. Such uncertainties will undermine the main findings of this work.

In the method section, we added following statement to explain why LCC is not included: "The main focus of this study is to quantify how the differences of anthropogenic emissions, including both CO_2 and air pollution which are usually associated, will cause different responses in land carbon budget to the same global warming target. Especially, the role of air pollution on land carbon cycle has always been ignored. The assumptions of land use can be quite uncertain among future pathways (Stehfest et al., 2019), and these assumptions are not necessarily associated with CO_2 and air pollution emissions. As a result, for this study, we consider fixed land cover in all simulations." (Lines 244-250)

CORRECTION: In the paper, we use –NBP from TRENDY to represent NEE (Fig. 4b). We noticed that we incorrectly use S3 instead of S2 for comparison in the original paper. In the revised paper, we use output of S2 (no LCC) for the evaluation of YIBs simulations and discuss the results accordingly.

Another concern is about scaling up leaf-scale co2 fixation to the canopy. How have the authors accounted for canopy layers and diffuse radiation produced within the canopy?

➔ We use the multi-layer canopy radiative transfer scheme proposed by Spitters (1986) to separate diffuse and direct radiation for sunlit and shaded leaves. The canopy is divided into an adaptive number of layers (typically 2-16) for light stratification. The sunlit leaves can receive both direct and diffuse radiation, while the shading leaves receive only diffuse radiation. The details of this scheme have been well documented in Yue and Unger (2017) and fully evaluated in Yue and Unger (2018). For this study, we refer readers to these references as follows: "Leaf-level photosynthesis is

calculated hourly using the well-established Farquhar et al. (1980) scheme and is upscaled to canopy level by the separation of sunlit and shading leaves (Spitters, 1986). Sunlit leaves can receive both direct and diffuse radiation, while shading leaves receive only the diffuse component (Yue and Unger, 2017)." (Lines 180-184) "Simulated GPP responses to direct and diffuse radiation show good agreement with observations at 24 global flux tower sites from FLUXNET network (Yue and Unger, 2018). In general, diffuse radiation is more efficient to enhance canopy photosynthesis compared to the same level of direct radiation." (Lines 210-213)

Also, the authors compiled experimental studies on ozone impacts on plants in China, based on which sensitivity of differing PFTs are assigned and a high and low sensitivity scheme is implemented. The variability of plant-ozone sensitivity is undeniable, which can go all the way down to the species level, evidenced by experimental studies across the globe. I am wondering what magnitude of uncertainty would such a PFT scheme bring to the quantification of GPP dampening by ozone.

➔ The uncertainties of ozone vegetation damaging are quantified using a low-to-high range of sensitivities for each individual PFT. Such range has been evaluated against available observations as shown in Fig. S4. In the revised text, we quantified and showed the uncertainties of ozone effects due to different damaging sensitivities: "In the present day, O_3 decreases GPP by 6.7±2.6% (uncertainties ranging from low to high damaging sensitivities) in China (Fig. 7d), because of the direct inhibition of photosynthesis by 6±2.4% (Fig. 7a) and the consequent reduction of 1.8±0.8% in leaf area index (LAI, Fig. 7g). For 1.5°C global warming, this weakening effect shows opposite tendencies in the two RCP scenarios, with a reduced GPP loss of 4.7±2.0% in RCP2.6 (Fig. 7e) but an increased loss of 7.9±3.0% in RCP8.5 (Fig. 7f). … Consequently, changes in O_3 help increase GPP by 0.1±0.03 Pg C yr^{-1} in RCP2.6 but decrease GPP by 0.14±0.04 Pg C yr^{-1} in RCP8.5 for the same 1.5°C warming. Following the benefits to GPP, the lower O_3 decreases NEE (strengthens the sink) by 0.06±0.02 Pg C yr^{-1} in RCP2.6, offsetting more than half of the negative effect (weakens the sink) from CO_2 (Fig. 6b)". (Lines 367-380)

Finally, a couple of spots of language errors are obvious: L64: changing 'in differing pathways' to 'of differing pathways' would be better. L164: 'respectively' should be added.

➔ Corrected as suggested.

Referee 2

In this manuscript, the authors use the YIBs model to simulate ecosystem productivity under two pathways to 1.5 C warming: and ensemble based on RCP2.6 and an ensemble based on RCP8.5. Overall, the 1.5 C warming is delayed by 30 years in RCP2.6, and results in weaker carbon sink overall on this pathway to 1.5 C. But the authors demonstrate that reductions air pollution emissions from RCP2.6 (resulting in increased light availability and decrease surface O3) is better for land carbon uptake compared to RCP8.5. The slower warming scenario from RCP2.6 increases the allowable anthropogenic carbon emissions.

This is a very interesting study that replaces the more familiar "temporal" domain for a "temperature" domain. This results in some initial awkwardness, since the different carbon sinks are not being compared at/over equivalent time periods, but the authors make a clear argument in their introduction for why they have chosen this approach, and why this experiment is a useful exercise. In general, I think some points of clarification would help this manuscript, as I outline below. Overall, this is a sound and novel study with results that should be of interest to the ACP audience.

➔ Thank you for your positive evaluations.

First, I would encourage the authors to explicitly describe how they have calculated NEE. While it is an obvious term to some, many of the readers in ACP may not find it as intuitive. If I have interpreted the authors work correctly (e.g. Figure 4 and its discussion), it seems like NEE is being calculated here as: NEE = – [GPP – Reco], where the authors have taken the convention that a negative NEE means a net carbon sink. I'm not sure why this equation isn't explicitly included somewhere, even if it might seem obvious. Actually, I couldn't find where the authors even define the abbreviation "NEE" (presumably "net ecosystem exchange"). Nor would I necessarily even expect ACP readers to be so well acquainted with the term "gross primary production" that this doesn't require an explanation/definition.

➔ Sorry for the missing information. We added definitions of GPP and NEE in the revised paper to clarify: "We focus on the changes of gross primary productivity (GPP) and net ecosystem exchange (NEE). GPP represents the total canopy photosynthesis through gross carbon assimilation. NEE is the residue after subtraction of GPP from ecosystem (plant plus soil) respiration (Reco – GPP), indicating the net carbon sink from land to atmosphere. The larger the GPP values, the stronger carbon assimilation by ecosystems. In contrast, the more negative the NEE, the stronger carbon sink of land." (Lines 83-88).

Without these definitions being explicitly laid out, things are in danger of becoming a bit unclear. For example, it might not be immediately obvious whether an "enhancement" in NEE is referring to a "more negative" value (and therefore a "stronger sink"). We run

into confusing instances such as that found in Line 316, referring to an "enhancement" in NEE of "0.03 Pg", which is somehow equivalent to a "-17%" difference. How can it be a simultaneously positive and negative difference, unless we know that enhancement refers to a more negative value? These instances could just use some clarification.

➔ In the revised text, we double checked that all the words "enhancement" or "enhance" are used only for GPP, not for NEE. For the descriptions mentioned above, we changed them as follows: "Projected NEE continues to be more negative in the RCP8.5 scenario after the year 2016 (Fig. S7b). Meanwhile, future NEE reaches the minimum value (or the maximum sink strength) around the year 2025 and then reverses to be less negative in the RCP2.6 scenario (Fig. S7b). By the period of 1.5°C global warming, NEE changes in China show opposite tendencies between the two pathways. Compared to the present day, NEE increases by 0.03 ± 0.03 Pg C yr^{-1} (-17.4±19.6 %) in RCP2.6 (Fig. 5d) but decreases by 0.14 ± 0.04 Pg C yr^{-1} (94.4±24.9 %) in RCP8.5 (Fig. 5e), suggesting that land carbon sink is slightly weakened in the former but strengthened in the latter." (Lines 329-337)

This clarification is especially important when the authors eventually start taking the differences in "NEE" between the two different pathways, further exacerbating the importance of keeping track of the sign convention. It isn't immediately obvious whether the authors are taking the difference of two negative numbers (E.g. (-1.5 – [-2]) = 0.5), or whether they are comparing absolute NEE values (i.e. so that in the hypothetical example above, (1.5 – 2) = -0.5). The choice is important since these deltas have opposite meanings! It is also possible I have misinterpreted the authors' approach. I encourage the authors to explicitly define all conventions, and repeat them appropriately, to help guide the reader.

➔ We carefully went through all descriptions related to changes in NEE and made following clarifications (underlined):

"The higher ΔGPP in RCP2.6 instead yields a weakened NEE (more positive) due to the CO_2 effects (Fig. 6b)" (Lines 352-353)
"Following the benefits to GPP, the lower O_3 decreases NEE (strengthens the sink) by 0.06±0.02 Pg C yr^{-1} in RCP2.6, offsetting more than half of the negative effect (weakens the sink) from CO_2 (Fig. 6b)." (Lines 378-380)
"Climate-induced ΔNEE is -0.02 Pg C yr^{-1} (strengthened sink) for both pathways (Fig. 6b)" (Lines 418-419)

We also flip y-axis of Figure 8 (see the end of this response) as suggested. The revised figure now shows carbon loss with positive numbers and carbon uptake (sink) with negative numbers, consistent with the sign of NEE.

Nevertheless, despite some of this awkwardness, I suppose the implications of the results are usually clear to the reader: E.g. improvements in air quality result in more light

availability and less ozone damage, which in turn drives a "better" land carbon uptake. (I would still encourage the authors to use clearer language than "better", see Line 399.)

➔ Yes, that's the main conclusion we achieved in this study. We removed the word "better" and revised the sentence as follows: "For a warming target of 1.5°C, our analyses suggest that a simultaneous reduction of CO_2 and air pollution emissions enhances the efficiency of land carbon uptake compared to a pathway without air pollution emission control." (Lines 424-426)

Specific comments:
Line 107: "We further remove…" Why is the word "further" here? Have the authors removed some models based on other criteria that weren't mentioned above?

➔ We deleted the word "further" to avoid confusions.

Line 138-139: "…apply the same protocols for anthropogenic and biomass burning emissions …" What do the authors mean by "same protocols?" Please be specific.

➔ The same protocols mean that these ACCMIP models all use the same anthropogenic and biomass burning emissions defined by CMIP5 RCP scenarios. In this case, the differences in the simulated air pollution originated from modeling structures and parameters, instead of emission inventories. To clarify, we revised this sentence as follows: "However, these models apply the same anthropogenic and biomass burning emissions specified for CMIP5 RCP scenarios (e.g., RCP2.6 or RCP8.5), though different models perform simulations at different time slices." (Lines 143-146)

Line 141-142: I'm curious about the approach used to account for the temporal gaps in O3 in the various ACCMIP models. The authors state they fill gaps using a linear fitting approach. Does this ignore seasonality? Or is it accounted for? This also means that Figure 3b is a bit misleading, since the ozone concentrations at some of these timeslices were not actually from any model output all, but from a very simple interpolation that might not capture multi-decade variability. For example, around the 2060 time slice of Figure 3b, I only see a couple of models in Table S3 that would actually have real output for this time slice. Most go from around 2030 to around 2090.

It seems to me that drawing a straight line between two time slices that are 70 years apart is a bit dubious, even if it doesn't change the direction of the overall conclusions. I think this limitation could be more explicitly mentioned/discussed. [Also: I see there must be a typo in the first row of Table S3, which says "2100-2019".]

➔ We retain the seasonality of ozone concentrations when interpolating ACCMIP data. Here, we use GFDL-AM3 model as an example (Fig. R2). The original model provides time slice simulations of 2001-2010 and 2031-2040. We perform linear interpolations for individual months. For example, we derive a linear fit using all the

July concentrations during 2001-2010 and 2031-2040, and then estimate July values within 2011-2030 based on this linear fit. Using the same method, we estimate ozone concentrations in all months individually so as to retain the seasonality of O_3.

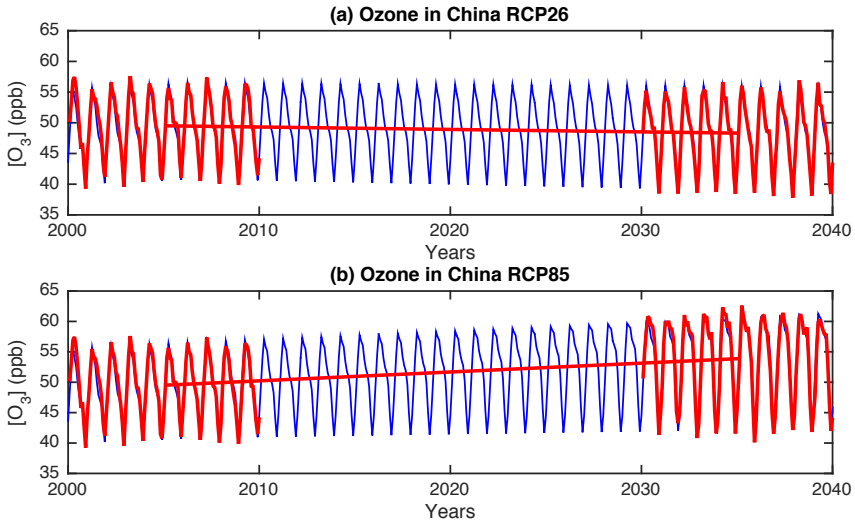

Fig. R2 Monthly ozone concentrations from GFDL-AM3 model for (a) RCP2.6 and (b) RCO8.5 scenarios. Time series from the original model are shown in red and the interpolations are shown in blue.

We agree that the linear interpolation may introduce some uncertainties in the gap filling. However, this is likely the best way we can consider in deriving unknown data. Other interpolation methods (e.g., polyfit, logfit) can also cause varied uncertainties. In addition, we believe that the multi-model ensemble average can in part smooth the data and achieve a reasonable time series of ozone concentrations that match the RCP emissions.

We corrected the typo in Table S3 (should be 2100-2109).

Line 284: "The YIBs simulations show variabilities of: : :" It wasn't immediately clear to me what the authors meant by "variabilities". It looks like they are referring to the full range of results from each YIBs ensemble?

➔ We explained that this variability is due to uncertainties in driven climate from CMIP5 models: "The YIBs simulations show variabilities of 0.41±0.23 Pg C yr^{-1} (6.2±3.9%, blue shading in Fig. 4a) due to uncertainties in climate from CMIP5 models" (Lines 299-301)

Line 334-340: I would have liked to see a more detailed discussion on the role of changes in ecosystem respiration on the difference in NEE between the two periods for each pathway. I had to spend a lot of time with Figure 6b to wrap my head around the "net"

difference between "net ecosystem exchange" at two different times, and how GPP and Reco must each play a role in this separately.

➔ We explained more details about changes in GPP and soil respiration, and their joint effects on NEE as follows: "The higher ΔGPP in RCP2.6 instead yields a weakened NEE (more positive) due to the CO_2 effects (Fig. 6b). The stabilization of CO_2 concentrations in this scenario (Fig. 3a) results in a stabilized GPP after the year 2040 (Fig. S7a). Meanwhile, the 55-year (from 2005 to 2060) carbon accumulation enhances soil carbon storage by 10.5±1.3 Pg C and promotes soil respiration to 0.71±0.19 Pg C yr^{-1}. The stabilized GPP while enhanced soil respiration (NEE = Reco – GPP, Reco includes both soil and plant respiration) together lead to a weakened carbon sink (less negative NEE) by 1.5°C warming period (Fig. 7b). In contrast, soil carbon storage increases only 5.2±0.5 Pg C in RCP8.5 due to relatively short time period (from 2005 to 2031) for carbon accumulation, leading to lower soil respiration of 0.41±0.15 Pg C yr^{-1} in the fast warming pathway. The continuous increase of GPP and lower soil respiration jointly strengthen the land carbon sink (more negative NEE) in China by 0.1 Pg C yr^{-1} under RCP8.5 scenario (Fig. 6a)." (Lines 352-364)

Figure 4: I wondered about also showing the YIBs future projections timeseries in this plot (or somewhere in the Supplemental material). I understand that the focus of this paper is in "temperature" space, instead of "temporal" space, but I just kept wondering what the projections actually looked like in the more familiar time x-axis. Obviously the RCP8.5 line would end earlier than the RCP2.6 line, but this might actually help clarify other points in the paper.

➔ We plotted the changes of GPP and NEE along the temporal axis and added it as Figure S7 in SI as suggested.

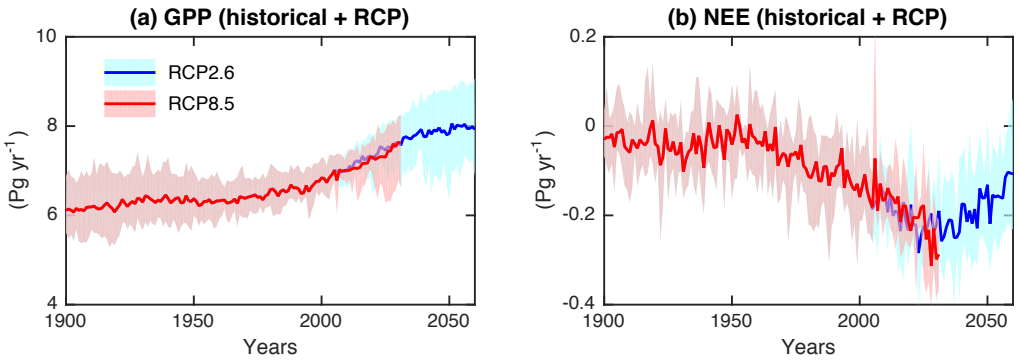

Figure S7. Projected historical and future carbon fluxes in China. Results shown are simulated (a) GPP and (b) net ecosystem exchange (NEE) during historical period (1901-2016) and future periods by 1.5ºC global warming (2017-2060 for RCP2.6 and 2017-2031 for RCP8.5). The bold lines are ensemble means with shadings for inter-vegetation-model uncertainties (blue for RCP2.6 and red for RCP8.5). All YIBs simulations are driven with daily meteorology from CMIP5 models.

We included following descriptions in the main text: "Projected GPP continues to increase in both RCP2.6 and RCP8.5 scenarios after the year 2016 (Fig. S7a)" (Lines 322-323) and "Projected NEE continues to be more negative in the RCP8.5 scenario after the year 2016 (Fig. S7b). Meanwhile, future NEE reaches the minimum value (or the maximum sink strength) around the year 2025 and then reverses to be less negative in the RCP2.6 scenario (Fig. S7b)." (Lines 329-332)

Figure 6: Should there be "delta" signs in the Y-axis label of these panels? This was a source of initial confusion for me.

➔ Corrected as suggested.

Figure 8: Here the signs could potentially be confusing again (in this case, positive refers to a land sink), although I guess the meaning is clear overall. It just doesn't seem consistent with the choices elsewhere in the paper. Also, I would encourage panel b to include the word "net" somewhere, although perhaps this implicit in the word "accumulated" and would just add to the confusion?

➔ We agree with the reviewer's comment that the original figure 8 may cause confusion due to the inconsistency of signs. In the revised paper, we flip around the y-axis to make the variables (either carbon loss or carbon sink) consistent with the sign of NEE. We also added the word "net" in the title of panel b as suggested.

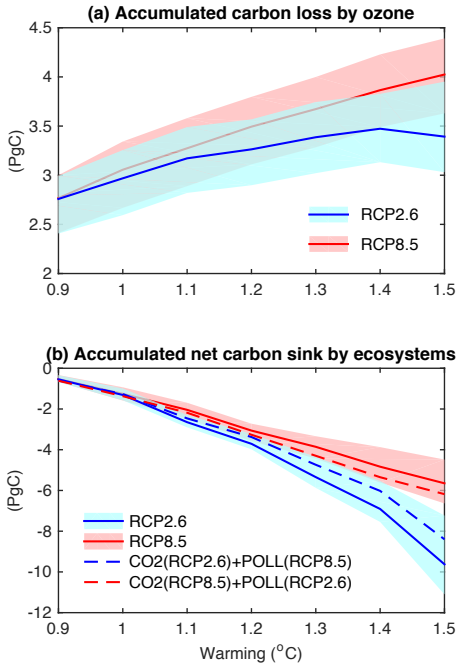

References

Chen, C., Park, T., Wang, X., Piao, S., Xu, B., Chaturvedi, R. K., Fuchs, R., Brovkin, V., Ciais, P., Fensholt, R., Tømmervik, H., Bala, G., Zhu, Z., Nemani, R. R., and Myneni, R. B.: China and India lead in greening of the world through land-use management, Nature Sustainability, 2, 122-129, 2019.

Farquhar, G. D., Caemmerer, S. V., and Berry, J. A.: A Biochemical-Model of Photosynthetic Co2 Assimilation in Leaves of C-3 Species, Planta, 149, 78-90, 10.1007/Bf00386231, 1980.

Spitters, C. J. T.: Separating the Diffuse and Direct Component of Global Radiation and Its Implications for Modeling Canopy Photosynthesis .2. Calculation of Canopy Photosynthesis, Agr Forest Meteorol, 38, 231-242, 10.1016/0168-1923(86)90061-4, 1986.

Stehfest, E., van Zeist, W. J., Valin, H., Havlik, P., Popp, A., Kyle, P., Tabeau, A., Mason-D'Croz, D., Hasegawa, T., Bodirsky, B. L., Calvin, K., Doelman, J. C., Fujimori, S., Humpenoder, F., Lotze-Campen, H., van Meijl, H., and Wiebe, K.: Key determinants of global land-use projections, Nat Commun, 10, 2166, 10.1038/s41467-019-09945-w, 2019.

Yue, X., and Unger, N.: Aerosol optical depth thresholds as a tool to assess diffuse radiation fertilization of the land carbon uptake in China, Atmospheric Chemistry and Physics, 17, 1329-1342, 10.5194/acp-17-1329-2017, 2017.

Yue, X., and Unger, N.: Fire air pollution reduces global terrestrial productivity, Nat Commun, 9, 5413, 10.1038/s41467-018-07921-4, 2018.

Pathway dependence of ecosystem responses in China to 1.5°C global warming

Xu Yue[1], Hong Liao[1], Huijun Wang[2], Tianyi Zhang[3], Nadine Unger[4], Stephen Sitch[4], Zhaozhong Feng[1] and Jia Yang[5]

[1] Jiangsu Key Laboratory of Atmospheric Environment Monitoring and Pollution Control, Collaborative Innovation Center of Atmospheric Environment and Equipment Technology, School of Environmental Science and Engineering, Nanjing University of Information Science & Technology (NUIST), Nanjing, 210044, China

[2] Ministry of Education Key Laboratory of Meteorological Disaster, Joint International Research Laboratory of Climate and Environment Change, Collaborative Innovation Center on Forecast and Evaluation of Meteorological Disasters, NUIST, Nanjing, 210044, China

[3] State Key Laboratory of Atmospheric Boundary Layer Physics and Atmospheric Chemistry, Institute of Atmospheric Physics, Chinese Academy of Sciences, Beijing, 100029, China

[4] College of Engineering, Mathematics and Physical Sciences, University of Exeter, Exeter, EX4 4QE, UK

[5] Department of Forestry, Mississippi State University, Mississippi State, MS, 39762, US

Email: yuexu@nuist.edu.cn and hongliao@nuist.edu.cn

Abstract

China is currently the world's largest emitter of both CO_2 and short-lived air pollutants. The ecosystems in China help mitigate a part of its carbon emissions, but are subject to perturbations in CO_2, climate, and air pollution. Here, we use a dynamic vegetation model and data from three model inter-comparison projects to examine ecosystem responses in China under different emission pathways towards the 1.5°C warming target set by the Paris Agreement. At 1.5°C warming, gross primary productivity (GPP) increases by 15.5±5.4 % in a stabilized pathway and 11.9±4.4 % in a transient pathway. CO_2 fertilization is the dominant driver of GPP enhancement and climate change is the main source of uncertainties. However, differences in ozone and aerosols explain the GPP differences between pathways at 1.5°C warming. Although the land carbon sink is weakened by 17.4±19.6 % in the stabilized pathway, the ecosystems mitigate 10.6±1.4% of national emissions in the stabilized pathway, more efficient than the fraction of 6.3±0.8% in the transient pathway. To achieve the 1.5°C warming target, our analysis suggests a higher allowable carbon budget for China under a stabilized pathway with reduced emissions in both CO_2 and air pollution.

Keywords: Ecosystems, climate change, 1.5°C warming, emission pathway, ozone vegetation damage

1 Introduction

The past decade has seen record-breaking warming largely related to anthropogenic greenhouse gas emissions (Mann et al., 2017). This warming trend presents a challenge to achieve the temperature control target of 1.5°C above the pre-industrial (PI) level set by the 2015 Paris climate agreement. Many studies have shown that a conservative warming such as 1.5°C is necessary to limit climatic extremes (Nangombe et al., 2018), avoid heat-related mortality (Mitchell et al., 2018), reduce economic loss(Burke et al., 2018), and alleviate ecosystem risks (Warszawski et al., 2013) compared to stronger anthropogenic warming. To achieve this target, each country must aim to control its greenhouse gas emissions. A full understanding of regional ecosystem response to the changing climate and environmental stress is essential to reduce uncertainties in allowable carbon budget estimates at 1.5°C (Mengis et al., 2018). China is covered with a wide range of terrestrial biomes (Fang et al., 2012). While China's ecosystem response to possible future climate has been explored (Wu et al., 2009;He et al., 2017;Dai et al., 2016), impacts on the regional carbon budget of differing pathways to the 1.5°C target are not known.

There are two distinct pathways to the 1.5°C global warming. One is a fast process in which global temperature passes 1.5°C and continues to increase (scenarios assuming high CO_2 emissions and no climate mitigation) while the other is a stabilized process with an equilibrium warming right below 1.5°C and last for decades before the end of 21st century (scenarios including climate mitigation). The stabilized pathway is the one proposed by the 2015 Paris agreement. However, the unprecedented warming in 2016 results in an increase of global average temperature by 1.1°C above PI (https://public.wmo.int), suggesting that the 1.5°C limit can be broken in a near future under a transient pathway. A few studies have compared allowable carbon budgets between these two pathways (Collins et al., 2018;Millar et al., 2017), but none has estimated the mitigation potential of regional ecosystems with joint impacts of changes in climate, CO_2, and air pollution under different pathways.

Deleted: ;He et al., 2017

Deleted: in

Deleted: Millar et al., 2017;

Here, we apply the Yale Interactive terrestrial Biosphere Model (YIBs) (Yue and Unger, 2015;Yue and Unger, 2018) to investigate the response of terrestrial ecosystem productivity in China to both stabilized and transient global warming of 1.5°C relative to PI period. We focus on the changes of gross primary productivity (GPP) and net ecosystem exchange (NEE). GPP represents the total canopy photosynthesis through gross carbon assimilation. NEE is the residue after subtraction of GPP from ecosystem (plant plus soil) respiration (Reco – GPP), indicating the net carbon sink from land to atmosphere. The larger the GPP values, the stronger carbon assimilation by ecosystems. In contrast, the more negative the NEE, the stronger carbon sink of land. The YIBs model is driven with meteorology from an ensemble of climate models in Climate Model Intercomparison Project Phase 5 (CMIP5). The stabilized global warming pathway is represented by the RCP2.6 low emissions scenario that yields an equilibrium change in Global Mean Temperature (ΔGMT) of 1.49°C by 2050-2070 with selected climate models (Fig. S1). The transient pathway is represented by RCP8.5 high emission scenario in which ΔGMT grows rapidly and realizes a transient 1.5°C around the year 2021-2041. We select the present-day period of 1995-2015 as a reference.

2 Methods

2.1 Datasets

2.1.1 CMIP5 data

We use both daily and monthly meteorology predicted by CMIP5 models (https://cmip.llnl.gov/). The daily data are used as input for YIBs model. In total, we select 15 climate models (Table S1) with all available daily meteorology, including surface air temperature, precipitation, specific humidity, surface downward shortwave radiation, surface pressure, and surface wind speed, for historical and two future scenarios (RCP2.6 and RCP8.5). These two scenarios assume distinct emission pathways of both CO_2 and air pollutants, with the RCP2.6 scenario projecting much lower CO_2 and pollution concentrations than RCP8.5. Simulated annual GMT is smoothed with a 21-year window to remove decadal variations. The ensemble changes

of GMT relative to PI period (1861-1900) from two scenarios are examined (Fig. S1a). The low emission scenario RCP2.6 yields an equilibrium ΔGMT of 1.85°C by 2100. We remove 8 climate models predicting stabilized ΔGMT higher than 1.85°C by the end of century. The 7 remaining models yield an ensemble warming close to 1.5°C (1.49°C for 2050-2070, Fig. S1b). Meanwhile, ΔGMT in the high emission scenario RCP8.5 grows fast and realizes a transient 1.5°C warming around the year 2021-2041. Daily meteorology from 7 selected models (Table S1) are then interpolated to the uniform 1°×1° resolution and used to drive YIBs model to simulate terrestrial carbon fluxes in China for 1850-2100. Due to the large data storage, we retain only the domain of [15-60ºN, 60-150ºE] covering China territory. We bias correct modeled meteorology with WFDEI (WATCH Forcing Data methodology applied to ERA-Interim reanalysis) data (Weedon et al., 2014):

$$V_d^s = V_d \times S_w / S_m \quad (1)$$

Here V_d is the original daily variables and V_d^s is the scaled value. S_w is the 2-dimensional WFDEI value averaged for 1980-2004 and S_m is the modeled values averaged at the same period. In this case, the average climate from each individual model matches observations at present day, meanwhile, climate variability from models are retained to estimate uncertainties in carbon fluxes.

2.1.2 TRENDY-v6 data

We acquire the global GPP and NEE datasets from 1901 to 2016 simulated by 14 Dynamic Global Vegetation Models (DGVMs) participating in TRENDY project (Table S2). All DGVMs are implemented following the same simulation protocol and driven by consistent input datasets, including CRU-NCEP climate data, atmospheric CO_2 concentrations, but fixed present-day land use (Le Quere et al., 2018).

2.1.3 ACCMIP O_3 data

We use monthly output of surface O_3 concentrations from 12 models joining the

Deleted: further

Atmospheric Chemistry and Climate Model Intercomparison Project (ACCMIP, Lamarque et al., 2013) (Table S3). The ACCMIP models have a wide range of horizontal and vertical resolutions, natural emissions, chemistry schemes, and interaction with radiation and clouds. However, these models apply the same anthropogenic and biomass burning emissions specified for CMIP5 RCP scenarios (e.g., RCP2.6 or RCP8.5), though different models perform simulations at different time slices. Here, we use surface O_3 and interpolate original output to 1°×1° resolution. We fill the temporal gaps between two adjacent time slices using a linear fitting approach. In this way, we derive the monthly O_3 from 1850 to 2100 for each model and their ensemble average at each grid point.

Deleted: they

Deleted: protocols for

Deleted: ,

2.1.4 Diffuse radiation data

The original CMIP5 archive does not provide diffuse component of shortwave radiation. Here, we use empirical relations between total and diffuse radiation from 11 studies to calculate hourly diffuse radiation (Table S4). The diffuse fraction k_d in all equations depends on clearness index k_t, which is defined as the ratio between global solar radiation I_t and extra-terrestrial solar radiation I_0 (Ghosh et al., 2017):

$$k_t = I_t / I_0 \quad (2)$$

$$I_0 = I_{sc}\left[1 + 0.033cos\left(\frac{360N}{365}\right)\right]cos\varphi \quad (3)$$

Here I_{sc} = 1367 W m^{-2} is solar constant, N is Julian day of the year, and φ is solar zenith. The empirical equations are evaluated using hourly total and diffuse radiation from Modern-Era Retrospective Analysis for Research and Applications (MERRA) (Rienecker et al., 2011) during 2008-2012. For each grid in China, we calculate hourly diffuse radiation (D_c) using MERRA total radiation and compare it with the standard output (D_m). Statistical metrics including correlation, normalized mean bias (NMB), and normalized root mean square error (NRMSE) are used to evaluate the performance of empirical equations:

$$\mathrm{NMB} = (\overline{D_c} - \overline{D_m})/\overline{D_m} \quad (4)$$

$$\mathrm{NRMSE} = \sqrt{\sum \frac{(D_c - D_m)^2}{n}}/\overline{D_m} \quad (5)$$

Here $\overline{D_c}$ and $\overline{D_m}$ are mean values of calculated and MERRA diffuse radiation, respectively. The evaluation is performed month by month for 2008-2012 and n is the number of daytime samples (grids with total radiation > 5 W m^{-2}). The value of n varies from month to month with a minimum of 540,000 in December 2010. Evaluation shows the empirical model M01 (Lam and Li, 1996) yields the highest correlation and the lowest NRMSE (Fig. S2). As a result, we use M01 model to derive diffuse radiation from CMIP5 models.

Deleted: .

2.2 Model

We apply the YIBs model (Yue and Unger, 2015;Yue et al., 2017) to simulate historical and future (1850-2100) ecosystem productivity. The YIBs model dynamically calculates LAI and tree height based on carbon assimilation and allocation. Leaf-level photosynthesis is calculated hourly using the well-established Farquhar et al. (1980) scheme and is upscaled to canopy level by the separation of sunlit and shading leaves (Spitters, 1986). Sunlit leaves can receive both direct and diffuse radiation, while shading leaves receive only the diffuse component (Yue and Unger, 2017). The assimilated carbon is in part used for maintenance and growth respiration, and the rest is allocated among leaf, stem, and root for plant growth (Clark et al., 2011). Soil respiration is calculated as the loss of carbon flows among 12 soil carbon pools (Schaefer et al., 2008). The YIBs model considers 9 plant functional types (PFTs) including evergreen needleleaf forest (ENF), deciduous broadleaf forest (DBF), evergreen broadleaf forest (EBF), shrubland, tundra, C3 grassland, C4 grassland, C3 cropland, and C4 cropland. The land cover is prescribed based on satellite retrievals from the Moderate Resolution Imaging Spectroradiometer (MODIS) (Hansen et al., 2003) and the Advanced Very High Resolution Radiometer (AVHRR) (Defries et al., 2000). For this study, we fix the land cover to isolate impacts of CO_2 and climatic changes. Other studies also show only moderate changes in vegetation fraction and composition at a low warming level (Warszawski et al., 2013). The YIBs model can be applied at the site, regional, and global scales. The site-level model has been evaluated with measured carbon fluxes from 145 FLUXNET sites (Yue and Unger, 2015). For

this study, all simulations are performed at the 1°×1° resolution over China. During the period of 1982-2011, YIBs predicts an average GPP of 7.17 Pg C yr^{-1} in China (Fig. S3), close to the 7.25 Pg C yr^{-1} estimated in the benchmark product (Jung et al., 2009).

YIBs model calculates O_3 damage to plant photosynthesis using a flux-based parameterization (Sitch et al., 2007). The inhibition rate of GPP is dependent on both ambient O_3 concentrations and stomatal conductance. Compared to hundreds of meta-analyses data from China (Table S5) and the world (Yue and Unger, 2018), the scheme shows good performance in estimating GPP responses to O_3 for DBF, EBF, C3 and C4 herbs (Fig. S4). The predicted O_3 damaging effects to ENF might be underestimated. The YIBs model separates the effects of diffuse and direct light on plant photosynthesis (Spitters, 1986). Simulated GPP responses to direct and diffuse radiation show good agreement with observations at 24 global flux tower sites from FLUXNET network (Yue and Unger, 2018). In general, diffuse radiation is more efficient to enhance canopy photosynthesis compared to the same level of direct radiation.

2.3 Simulations

We perform two main groups of simulations, one for RCP2.6 and the other for RCP8.5. For each group, 7 sub-groups are designed with varied climatic or CO_2 forcings (Table S6). In each sub-group, separate runs are conducted for the YIBs model driven with climate variables from 7 selected CMIP5 models (Table S1), making a total of 98 runs. A baseline group (HIST_2000) is perform with fixed meteorology and CO_2 after the year 2000. Another four sub-group simulations are performed to quantify O_3 effects on photosynthesis (Table S7). These simulations are driven with both CMIP5 meteorology and monthly O_3 concentrations from an ensemble of 12 ACCMIP models. The runs are distinguished with different O_3 damaging sensitivity (high or low) and scenario projections (RCP2.6 or RCP8.5). Monthly O_3 concentrations are downscaled to hourly step using the diurnal cycle simulated by a chemistry-climate model NASA ModelE2 (Schmidt et al., 2014). The O_3-affected GPP or NEE are calculated as the average of simulations with low and high sensitivities.

For each run, a 251-year simulation is performed with historical climate for 1850-2000 and future climate for 2001-2100. For simulations driven with meteorology from the same climate model, all sensitivity tests apply the same climate forcing during historical period but utilize varied forcings after the year 2000. For example, RCP26_CO2 is identical to RCP26_MET for the period of 1850-2000. However, after the year 2000, the former runs fix climatic conditions at the year 2000 but allow changes in CO_2 concentrations year by year for 2001-2100 following the pathway projection, while the latter fix CO_2 level at the year 2000 but continue to use day-to-day meteorology after 2000. For all simulations, we initialize vegetation and soil carbon pools in the YIBs model with a 200-year spin up by recycling meteorology at the year of 1850. Contributions of individual factors are calculated as the differences between sensitivity and baseline group (e.g., RCP26_CO2 – HIST_2000 for CO_2 fertilization in RCP2.6 scenario).

The main focus of this study is to quantify how the differences of anthropogenic emissions, including both CO_2 and air pollution which are usually associated, will cause different responses in land carbon budget to the same global warming target. Especially, the role of air pollution on land carbon cycle has always been ignored. The assumptions of land use can be quite uncertain among future pathways (Stehfest et al., 2019), and these assumptions are not necessarily associated with CO_2 and air pollution emissions. As a result, for this study, we consider fixed land cover in all simulations.

3 Results

3.1 Changes of atmospheric compositions and radiation

The ensemble concentrations of ACCMIP O_3 show good agreement with ground-based observations from 1580 sites in China (Fig. 1). The spatial correlation is R=0.80 (p < 0.01) between observations and the ensemble O_3 concentrations ([O_3]), though the latter is higher by 25% (Figs. 1a-1c). Such overestimation is likely attributed to the high [O_3] at night in the models, because the evaluation of maximum daily 8-hour average

(MDA8) [O_3], which mainly occurs in the daytime, shows more reasonable predictions with a lower bias of 10% (Figs. 1d-1f). Since the O_3 vegetation damage in general occurs in the daytime, when both plant photosynthesis and [O_3] are at high levels, the ACCMIP [O_3] is good to be used as input for YIBs model to derive long-term O_3 inhibition effects on ecosystem productivity.

The ensemble radiation from CMIP5 models matches observations at 106 sites in China (Fig. 2). For total shortwave radiation, the model prediction shows high values in the West and low values in the Southeast, consistent with observations for a correlation coefficient of $R = 0.79$ ($p < 0.01$) and a mean bias of 8.9%. The derived diffuse radiation is highest in the Southeast, where the total radiation is lowest. Observed diffuse radiation is available only at 17 sites. Compared to these sites, predictions show reasonable spatial distribution with a correlation of $R = 0.65$ ($p < 0.01$) and a low bias of 7.1%. Both the total radiation and derived diffuse radiation are used as input for YIBs model to estimate GPP responses to joint changes in direct and diffuse radiation caused by aerosol removal.

Atmospheric compositions and radiation show varied changes in different scenarios. The GMT changes mainly follow those in CO_2 concentrations, which show fast growth in RCP8.5 but slow changes in RCP2.6 (Fig. 3a). The latter assumes a large reduction of carbon emissions globally after the year 2020 (Meinshausen et al., 2011). Global CO_2 levels reduce slightly after the year 2030 in RCP2.6, while GMT continues growing until 2050 due to air-sea interactions (Solomon et al., 2009). As a low emission scenario, RCP2.6 experiences a slow growth in nitrogen oxide (NO_x) emissions and a continuous reduction after the year 2020 (Fig. S5), resulting in a decline of 6.4 ppb (15.2%) in surface O_3 over eastern China by 1.5°C warming at 2060 (Fig. 3b). In contrast, RCP8.5 assumes fast growth of NO_x emissions with delayed controls after the year 2030, leading to surface O_3 enhancements of 6.6 ppb (15.7%) by 1.5°C warming at 2030. The lower emissions in RCP2.6 also result in smaller aerosol optical depth (AOD) than RCP8.5 (Fig. S6), leading to higher surface total radiation (Fig. 3c) while

lower diffuse radiation (Fig. 3d) due to reducing light extinction (Yu et al., 2006).

3.2 Historical ecosystem productivity in China

The ensemble simulations show an increasing trend in GPP in China of 0.011 Pg C yr^{-2} over the historical period, 1901-2016 (Fig. 4a). A stronger trend of 0.022 Pg C yr^{-2} is found after 1960. Such change is much faster than the trend of 0.013 Pg C yr^{-2} estimated by a benchmark product (Jung et al., 2009) for 1982-2011 but close to a recent estimate of 0.02 Pg C yr^{-2} combining machine learning algorithms and eddy flux measurements from 40 sites in China (Yao et al., 2018). Simulated trend is also consistent with the TRENDY ensemble, which predicts trends of 0.013 ± 0.006 Pg C yr^{-2} (ensemble ± inter-model uncertainty) for 1901-2016 and 0.022 ± 0.01 Pg C yr^{-2} for 1961-2016. The YIBs simulations show variabilities of 0.41±0.23 Pg C yr^{-1} (6.2±3.9%, blue shading in Fig. 4a) due to uncertainties in climate from CMIP5 models, much smaller than the value of 1.33±0.16 Pg C yr^{-1} (19.2±2.6%, red shading in Fig. 4a) caused by structural uncertainties across different vegetation models.

NEE in China is negative, suggesting a regional land carbon sink (Fig. 4b). This sink is -94.7 Tg C yr^{-1} with a trend of -1.7 Tg C yr^{-2} during 1901-2016. Such change matches TRENDY simulations, which predict a multi-model mean carbon sink of -74.1±30.8 Tg C yr^{-1} (uncertainties due to inter-model variations) and a trend of -1.3±0.7 Tg C yr^{-2} for the same period. During 1980-1989, the ground-based estimate (Piao et al., 2009) suggests a sink of 177±73 Tg C yr^{-1} in China, consistent with the sink intensity of 149±20 Tg C yr^{-1} from the YIBs ensemble prediction. For the recent period of 1980-2000, YIBs estimates a strengthened sink of 154±30 Tg C yr^{-1} in China, weaker than the estimate of 198±114 Tg C yr^{-1} with the DLEM vegetation model (Tian et al., 2011) but is within the estimates of 137-177 Tg C yr^{-1} based on both ground and satellite data (Fang et al., 2007). The interannual variability in YIBs simulations is much weaker than the estimates in other studies, because the ensemble approach largely dampen variations among different runs. Similar to GPP, the NEE simulations exhibit smaller variability of 62±50 Tg C yr^{-1} among different YIBs runs than that of 122±57 Tg C yr^{-1} among

Deleted: gross primary productivity (

Deleted:)

Deleted: Net ecosystem exchange (

Deleted:)

Deleted: moderate at -46.3

Deleted: before 1960 but shows

Deleted: strong

Deleted: 3.

Deleted: thereafter

Deleted: weak

Deleted: 2 Tg C yr

Formatted: Not Superscript/ Subscript

Deleted: before 1960

Deleted: strengthened

Deleted: .2±2.8

Deleted: 1961-2016. However, TRENDY predicts ensemble sources of 41.3 Tg C yr^{-1} for 1915-1930 and 25.6 Tg C yr^{-1} for

Deleted: , both of which are missing in the YIBs simulations. For the latter period

Deleted: 128±88

different TRENDY models.

3.3 Future changes of carbon fluxes

Projected GPP continues to increase in both RCP2.6 and RCP8.5 scenarios after the year 2016 (Fig. S7a). By the global warming of 1.5°C, GPP increases significantly in China, especially over eastern and northeastern parts (Fig. 5). Compared to the present day, GPP with O_3 effects increases by 1.07 ± 0.38 Pg C yr^{-1} (15.5 ± 5.4 %) in the RCP2.6 scenario (Fig. 5a) and 0.82 ± 0.30 Pg C yr^{-1} (11.9 ± 5.4%) in RCP8.5 (Fig. 5b). The spatial pattern of the GPP changes is similar in the two pathways (correlation coefficient R=0.93), except that ΔGPP in RCP2.6 is higher than in RCP8.5 by 30% with a positive center over eastern China (Fig. 5c). Projected NEE continues to be more negative in the RCP8.5 scenario after the year 2016 (Fig. S7b). Meanwhile, future NEE reaches the minimum value (or the maximum sink strength) around the year 2025 and then reverses to be less negative in the RCP2.6 scenario (Fig. S7b). By the period of 1.5°C global warming, NEE changes in China show opposite tendencies between the two pathways. Compared to the present day, NEE increases by 0.03 ± 0.03 Pg C yr^{-1} (-17.4±19.6 %) in RCP2.6 (Fig. 5d) but decreases by 0.14 ± 0.04 Pg C yr^{-1} (94.4±24.9 %) in RCP8.5 (Fig. 5e), suggesting that land carbon sink is slightly weakened in the former but strengthened in the latter. Their differences exhibit widespread positive values in China with high centers in the East (Fig. 5f).

The changes in carbon fluxes follow the variations in atmospheric composition and climate (Fig. 6 and Figs. S8-S11). By the global warming of 1.5°C, a dominant fraction of GPP enhancement in China is attributed to CO_2 fertilization (Fig. 6a). For the RCP2.6 scenario, CO_2 alone contributes 0.83 Pg C yr^{-1} (77%) to ΔGPP, with the highest enhancement of 0.8 g C m^{-2} day^{-1} over the southeast coast (Fig. S8a). For RCP8.5, CO_2 fertilization increases GPP by 0.95 Pg C yr^{-1}, even higher than the total ΔGPP of 0.82 Pg C yr^{-1}. The larger CO_2-induced ΔGPP in RCP8.5 is due to the higher CO_2 concentrations (454 ppm) than RCP2.6 (442 ppm) at the same 1.5°C warming (Fig. 3a). The 12 ppm differences in CO_2 concentrations lead to a change of 0.12 Pg C yr^{-1} (1.7%)

Deleted: For a

Deleted: The

Formatted: Font color: Text 1

Deleted: a global warming of 1.5°C enhances NEE

Deleted: reduces NEE

Deleted: S7-S10

Deleted: S7a

in GPP. This sensitivity of GPP to CO_2, 0.14% ppm^{-1}, falls within the range of 0.05-0.21% ppm^{-1} as predicted by 10 terrestrial models (Piao et al., 2013) and that of 0.01-0.32% ppm^{-1} as observed from multiple free-air CO_2 enrichment (FACE) sites (Ainsworth and Long, 2005). The higher ΔGPP in RCP2.6 instead yields a weakened NEE (more positive) due to the CO_2 effects (Fig. 6b). The stabilization of CO_2 concentrations in this scenario (Fig. 3a) results in a stabilized GPP after the year 2040 (Fig. S7a). Meanwhile, the 55-year (from 2005 to 2060) carbon accumulation enhances soil carbon storage by 10.5±1.3 Pg C and promotes soil respiration to 0.71±0.19 Pg C yr^{-1}. The stabilized GPP while enhanced soil respiration (NEE = Reco – GPP, Reco includes both soil and plant respiration) together lead to a weakened carbon sink (less negative NEE) by 1.5°C warming period (Fig. 7b). In contrast, soil carbon storage increases only 5.2±0.5 Pg C in RCP8.5 due to relatively short time period (from 2005 to 2031) for carbon accumulation, leading to lower soil respiration of 0.41±0.15 Pg C yr^{-1} in the fast warming pathway. The continuous increase of GPP and lower soil respiration jointly strengthen the land carbon sink (more negative NEE) in China by 0.1 Pg C yr^{-1} under RCP8.5 scenario (Fig. 6a).

Ozone (O_3) damages plant photosynthesis and the land carbon sink (Sitch et al., 2007;Yue and Unger, 2018). In the present day, O_3 decreases GPP by 6.7±2.6% (uncertainties ranging from low to high damaging sensitivities) in China (Fig. 7d), because of the direct inhibition of photosynthesis by 6±2.4% (Fig. 7a) and the consequent reduction of 1.8±0.8% in leaf area index (LAI, Fig. 7g). For 1.5°C global warming, this weakening effect shows opposite tendencies in the two RCP scenarios, with a reduced GPP loss of 4.7±2.0% in RCP2.6 (Fig. 7e) but an increased loss of 7.9±3.0% in RCP8.5 (Fig. 7f). These impacts are predominantly driven by the variations of surface O_3 concentrations in the two scenarios, as predicted O_3 at 1.5°C warming decreases by 15.2% in the low emission pathway but increases by 15.7% in the high emission pathway (Fig. 3b). Consequently, changes in O_3 help increase GPP by 0.1±0.03 Pg C yr^{-1} in RCP2.6 but decrease GPP by 0.14±0.04 Pg C yr^{-1} in RCP8.5 for the same 1.5°C warming. Following the benefits to GPP, the lower O_3 decreases

Deleted: , while
Deleted: 1995-2015
Deleted: 2050-2070)
Deleted: of
Deleted: continues promoting
Deleted: , much higher than the value
Deleted: RCP8.5 from
Deleted: 26-year (to 2021-2041) carbon uptake.
Deleted: CO_2
Deleted: %

NEE (strengthens the sink) by 0.06±0.02 Pg C yr^{-1} in RCP2.6, offsetting more than half of the negative effect (weakens the sink) from CO_2 (Fig. 6b). For RCP8.5, O_3 impacts make limited contributions to ΔNEE.

Changes in meteorology account for the rest of the perturbations in the carbon fluxes. At the global warming of 1.5°C, temperature in China increases by 0.90°C for RCP2.6 and 0.91°C for RCP8.5 (Figs. S12a-S12b) compared to present-day climate. The spatial pattern of these changes is very similar without significant differences (Fig. S12c), leading to almost identical GPP responses (Figs. S8d and S9d). Generally, higher temperature is not beneficial for plant photosynthesis at low latitudes (Piao et al., 2013), where regional summer climate is already warmer than the optimal temperature threshold for leaf photosynthesis (Corlett, 2011). As a result, warming leads to negative changes in GPP over the East. Surface specific humidity exhibits widespread enhancement in eastern China (Figs. S13a-S13b). Air humidity may rise in a warmer climate because the corresponding enhancement of saturation pressure allow atmosphere to hold more water vapor. On average, surface specific humidity increases by 0.34 g kg^{-1} in RCP2.6 and 0.31 g kg^{-1} in RCP8.5, leading to a promotion of GPP by 0.14 Pg C yr^{-1} in the former and a similar value of 0.12 Pg C yr^{-1} in the latter (Figs. S8e and S9e). Precipitation increases by 0.14 mm day^{-1} (4.6%) over eastern China in RCP2.6 but decreases by 0.03 mm day^{-1} (1.2%) in RCP8.5 (Figs. S12d-S12e), leading to higher soil moisture in eastern China for RCP2.6 (Figs. S13d-S13e). Nevertheless, most of vegetation in eastern China is not water stressed, leaving moderate GPP responses to soil moisture changes in both RCP scenarios (Figs. S8f and S9f).

For the RCP2.6 scenario, the net effect of climate change causes an increase of 0.15 Pg C yr^{-1} in GPP with a range from -0.54 to 0.62 Pg C yr^{-1} (Fig. 6a). Such large variability in ΔGPP is related to the uncertainties in meteorology from different climate models. For RCP8.5, climate-induced GPP change is only 0.04 Pg C yr^{-1} with a range from -0.6 to 0.26 Pg C yr^{-1}. The discrepancy of ΔGPP for the two pathways is mainly caused by the different radiation impacts, which enhance GPP by 0.2 Pg C yr^{-1} in RCP2.6 but only

Deleted: S11a-S11b
Deleted: S11c
Deleted: S7d
Deleted: S8d
Deleted: S12a-S12b
Deleted: S7e
Deleted: S8e
Deleted: S11d-S11e
Deleted: S12d-S12e
Deleted: S7f
Deleted: S8f

0.11 Pg C yr^{-1} in RCP8.5 (Fig. 6a). Photosynthetically active radiation (PAR) is higher by 2.8 W m^{-2} in RCP2.6 than in RCP8.5 (Fig. 3c). The distinct changes in radiation are related to aerosol radiative effects, because global analyses also show radiation enhancement in regions (e.g., U.S. and Europe) with aerosol removal (Fig. S14). The lower AOD in RCP2.6 helps increase solar insolation at surface by reducing light extinction (Yu et al., 2006), and promote precipitation with weaker aerosol semi-direct and indirect effects (Lohmann and Feichter, 2005). Although lower aerosols in RCP2.6 slightly decrease diffuse radiation (Fig. 3d), which is more efficient in increasing photosynthesis (Mercado et al., 2009;Yue and Unger, 2018), the overall enhancement in total radiation helps boost GPP. Climate-induced ΔNEE is -0.02 Pg C yr^{-1} (strengthened sink) for both pathways (Fig. 6b), resulting from comparable responses of NEE to changes in radiation (R=0.82), temperature (R=0.71), air humidity (R=0.91), and soil moisture (R=0.73) between the two pathways (Figs. S10 and S11).

Deleted: S13

Deleted: S9

Deleted: S10

3.4 Impacts on allowable carbon budget

For a warming target of 1.5°C, our analyses suggest that a simultaneous reduction of CO_2 and air pollution emissions enhances the efficiency of land carbon uptake compared to a pathway without air pollution emission control. The increased light availability from aerosol removal and decreased surface O_3 jointly promote GPP in China by 0.3 Pg C yr^{-1}, equivalent to 36% of the CO_2 fertilization. In contrast, air pollution results in a net GPP inhibition of 0.03 Pg C yr^{-1} under the high emission pathway, suggesting a detrimental environment for plant health. Compared to RCP8.5, the timing of 1.5°C warming is delayed by 30 years in RCP2.6, leading to weaker carbon sink in the latter. However, even with the longer period of accumulation, the total carbon loss by O_3 damage is smaller by 3-16% in RCP2.6 relative to RCP8.5 at the same warming level (Fig. 8a).

Deleted: is better for

Deleted: than

The slow warming increases the allowable cumulative anthropogenic carbon emissions. Assuming China's carbon emission fraction of 27% of the world (the level at year 2017) (Le Quere et al., 2018), the total national emissions allowed are 80.4 Pg C in RCP2.6

and 71.9 Pg C in RCP8.5 from the year 2010 to the 1.5°C warming, following the global emission rates defined for these scenarios. The ensemble simulations show that ecosystems in China help mitigate 8.5±1.1 Pg C in RCP2.6 and 4.5±0.6 Pg C in RCP8.5 (Fig. 8b). Sensitivity experiments with either reduced CO_2 (but retain high pollution) or reduced pollution (but retain high CO_2) reveal land carbon uptakes of 7.3±0.9 Pg C and 5.0±0.6 Pg C, respectively. These values are both lower than that in RCP2.6, suggesting that simultaneous control of carbon and air pollution emissions can maximize the mitigation potential of ecosystems. The higher ecosystem assimilation rate in a low emission pathway (10.6±1.4% in RCP2.6 vs. 6.3±0.8% in RCP8.5) over China, which is not considered in CMIP5 models, further buffers the pace to the global warming of 1.5°C.

4 Discussion and conclusions

Projection of future ecosystem productivity is subject to uncertainties in climate forcing and biophysical responses. The multi-model ensemble is a good approach to reduce the uncertainty in climate (Flato et al., 2013). In this study, we employ daily meteorology from 7 CMIP5 models. A comparison with more CMIP5 models is performed (not shown) and confirms that the changes in meteorology from the 7 selected climate models are robust and representative of future projections. As for ecosystem responses, future projections generally showed increasing GPP in China (Mu et al., 2008;Ji et al., 2008;Ju et al., 2007), however, climate change alone usually reduces productivity by inducing hot and drought weather conditions. In contrast, the YIBs simulations reveal a net positive effect of climate change on GPP though with large uncertainties (Fig. 6a). Such discrepancies are related to structural uncertainties across different vegetation models. Evaluations suggest that biophysical responses to environmental forcings in the YIBs model are generally reasonable as compared to the TRENDY ensemble (Fig. 4).

Deleted: ;Ji et al., 2008;Mu et al., 2008

The YIBs simulations do not consider nitrogen cycle and its limitation on carbon uptake. Inter-model comparisons show that models without nutrient constraints tend to

overestimate GPP responses to CO_2 fertilization (Smith et al., 2016). As a result, the difference of CO_2 contributions in RCP scenarios would be smaller than predicted (Fig. 6a), suggesting that GPP enhancement in RCP2.6 might be even higher than RCP8.5 if nitrogen cycle is included. In contrast, nitrogen deposition in RCP2.6 would be much smaller than that in RCP8.5 due to emission control (Fig. S5), leading to lower nitrogen supply for ecosystem in the former scenario. Consequently, plant photosynthesis is confronted with stronger nutrient limit in RCP2.6 than that in RCP8.5, resulting in lower CO_2 fertilization efficiency in the former scenario. The net effect of nitrogen cycle on land carbon cycle is very uncertain (Zaehle et al., 2014;Huntzinger et al., 2017;Xiao et al., 2015).

For a warming target of 1.5°C, our analyses suggest that an associated reduction of CO_2 and pollution emissions brings more benefits to ecosystems in China than a pathway without emission control. The slow changes of temperature and other environmental variables due to slow growth of CO_2 are helpful for plant adaptation and limit biome shift (Warszawski et al., 2013), and the lower O_3 and higher solar radiation from aerosol removal increase plant photosynthesis. Consequently, China's ecosystems mitigate 10.6±1.4% of national emissions in the stabilized pathway, more efficient than the fraction of 6.3±0.8% in the transient pathway, leaving more allowable carbon budget for economic development and upgrade.

Deleted: Xiao et al., 2015;

Deleted:

References

Ainsworth, E. A., and Long, S. P.: What have we learned from 15 years of free-air CO2 enrichment (FACE)? A meta-analytic review of the responses of photosynthesis, canopy, New Phytol, 165, 351-371, 10.1111/J.1469-8137.2004.01224.X, 2005.

Burke, M., Davis, W. M., and Diffenbaugh, N. S.: Large potential reduction in economic damages under UN mitigation targets, Nature, 557, 549-553, 10.1038/s41586-018-0071-9, 2018.

Clark, D. B., Mercado, L. M., Sitch, S., Jones, C. D., Gedney, N., Best, M. J., Pryor, M., Rooney, G. G., Essery, R. L. H., Blyth, E., Boucher, O., Harding, R. J., Huntingford, C., and Cox, P. M.: The Joint UK Land Environment Simulator (JULES), model description - Part 2: Carbon fluxes and vegetation dynamics, Geosci Model Dev, 4, 701-722, 10.5194/Gmd-4-701-2011, 2011.

Collins, W. J., Webber, C. P., Cox, P. M., Huntingford, C., Lowe, J., Sitch, S., Chadburn, S. E., Comyn-Platt, E., Harper, A. B., Hayman, G., and Powell, T.: Increased importance of methane reduction for a 1.5 degree target, Environ Res Lett, 13, 054003, 10.1088/1748-9326/aab89c, 2018.

Corlett, R. T.: Impacts of warming on tropical lowland rainforests, Trends Ecol Evol, 26, 606-613, 10.1016/j.tree.2011.06.015, 2011.

Dai, E. F., Wu, Z., Ge, Q. S., Xi, W. M., and Wang, X. F.: Predicting the responses of forest distribution and aboveground biomass to climate change under RCP scenarios in southern China, Global Change Biol, 22, 3642-3661, 10.1111/gcb.13307, 2016.

Defries, R. S., Hansen, M. C., Townshend, J. R. G., Janetos, A. C., and Loveland, T. R.: A new global 1-km dataset of percentage tree cover derived from remote sensing, Global Change Biol, 6, 247-254, 10.1046/J.1365-2486.2000.00296.X, 2000.

Fang, J. Y., Guo, Z. D., Piao, S. L., and Chen, A. P.: Terrestrial vegetation carbon sinks in China, 1981-2000, Sci China Ser D, 50, 1341-1350, 10.1007/s11430-007-0049-1, 2007.

Fang, J. Y., Shen, Z. H., Tang, Z. Y., Wang, X. P., Wang, Z. H., Feng, J. M., Liu, Y. N., Qiao, X. J., Wu, X. P., and Zheng, C. Y.: Forest community survey and the structural characteristics of forests in China, Ecography, 35, 1059-1071, 10.1111/j.1600-0587.2013.00161.x, 2012.

Farquhar, G. D., Caemmerer, S. V., and Berry, J. A.: A Biochemical-Model of Photosynthetic Co2 Assimilation in Leaves of C-3 Species, Planta, 149, 78-90, 10.1007/Bf00386231, 1980.

Flato, G., Marotzke, J., Abiodun, B., Braconnot, P., Chou, S. C., Collins, W., Cox, P., Driouech, F., Emori, S., Eyring, V., Forest, C., Gleckler, P., Guilyardi, E., Jakob, C., Kattsov, V., Reason, C., and Rummukainen, M.: Evaluation of Climate Models, in: Climate Change 2013: The Physical Science Basis. Contribution of Working Group I to the Fifth Assessment Report of the Intergovernmental Panel on Climate Change, edited by: Stocker, T. F., Qin, D., Plattner, G. K., Tignor, M., Allen, S. K., Boschung, J., Nauels, A., Xia, Y., Bex, V., and Midgley, P. M., Cambridge University Press, Cambridge, United Kingdom and New York, NY, USA, 2013.

Ghosh, A., Norton, B., and Duffy, A.: Effect of sky clearness index on transmission of evacuated (vacuum) glazing, Renewable Energy, 105, 160-166, 10.1016/j.renene.2016.12.056, 2017.

Hansen, M. C., DeFries, R. S., Townshend, J. R. G., Carroll, M., Dimiceli, C., and Sohlberg, R. A.: Global Percent Tree Cover at a Spatial Resolution of 500 Meters: First Results of the MODIS Vegetation Continuous Fields Algorithm, Earth Interact, 7, 1-15, 10.1175/1087-3562(2003)007<0001:GPTCAA>2.0.CO;2, 2003.

He, N. P., Wen, D., Zhu, J. X., Tang, X. L., Xu, L., Zhang, L., Hu, H. F., Huang, M., and Yu, G. R.: Vegetation carbon sequestration in Chinese forests from 2010 to 2050, Global Change Biol,

23, 1575-1584, 10.1111/gcb.13479, 2017.
Huntzinger, D. N., Michalak, A. M., Schwalm, C., Ciais, P., King, A. W., Fang, Y., Schaefer, K., Wei, Y., Cook, R. B., Fisher, J. B., Hayes, D., Huang, M., Ito, A., Jain, A. K., Lei, H., Lu, C., Maignan, F., Mao, J., Parazoo, N., Peng, S., Poulter, B., Ricciuto, D., Shi, X., Tian, H., Wang, W., Zeng, N., and Zhao, F.: Uncertainty in the response of terrestrial carbon sink to environmental drivers undermines carbon-climate feedback predictions, Scientific Reports, 7, 4765, 10.1038/s41598-017-03818-2, 2017.
Ji, J. J., Huang, M., and Li, K. R.: Prediction of carbon exchanges between China terrestrial ecosystem and atmosphere in 21st century, Sci China Ser D, 51, 885-898, 10.1007/s11430-008-0039-y, 2008.
Ju, W. M., Chen, J. M., Harvey, D., and Wang, S.: Future carbon balance of China's forests under climate change and increasing CO2, J Environ Manage, 85, 538-562, 10.1016/j.jenvman.2006.04.028, 2007.
Jung, M., Reichstein, M., and Bondeau, A.: Towards global empirical upscaling of FLUXNET eddy covariance observations: validation of a model tree ensemble approach using a biosphere model, Biogeosciences, 6, 2001-2013, 10.5194/bg-6-2001-2009, 2009.
Lam, J. C., and Li, D. H. W.: Correlation between global solar radiation and its direct and diffuse components, Build Environ, 31, 527-535, 10.1016/0360-1323(96)00026-1, 1996.
Lamarque, J. F., Shindell, D. T., Josse, B., Young, P. J., Cionni, I., Eyring, V., Bergmann, D., Cameron-Smith, P., Collins, W. J., Doherty, R., Dalsoren, S., Faluvegi, G., Folberth, G., Ghan, S. J., Horowitz, L. W., Lee, Y. H., MacKenzie, I. A., Nagashima, T., Naik, V., Plummer, D., Righi, M., Rumbold, S. T., Schulz, M., Skeie, R. B., Stevenson, D. S., Strode, S., Sudo, K., Szopa, S., Voulgarakis, A., and Zeng, G.: The Atmospheric Chemistry and Climate Model Intercomparison Project (ACCMIP): overview and description of models, simulations and climate diagnostics, Geosci Model Dev, 6, 179-206, 10.5194/gmd-6-179-2013, 2013.
Le Quere, C., Andrew, R. M., Friedlingstein, P., Sitch, S., Pongratz, J., Manning, A. C., Korsbakken, J. I., Peters, G. P., Canadell, J. G., Jackson, R. B., Boden, T. A., Tans, P. P., Andrews, O. D., Arora, V. K., Bakker, D. C. E., Barbero, L., Becker, M., Betts, R. A., Bopp, L., Chevallier, F., Chini, L. P., Ciais, P., Cosca, C. E., Cross, J., Currie, K., Gasser, T., Harris, I., Hauck, J., Haverd, V., Houghton, R. A., Hunt, C. W., Hurtt, G., Ilyina, T., Jain, A. K., Kato, E., Kautz, M., Keeling, R. F., Goldewijk, K. K., Kortzinger, A., Landschutzer, P., Lefevre, N., Lenton, A., Lienert, S., Lima, I., Lombardozzi, D., Metzl, N., Millero, F., Monteiro, P. M. S., Munro, D. R., Nabel, J. E. M. S., Nakaoka, S., Nojiri, Y., Padin, X. A., Peregon, A., Pfeil, B., Pierrot, D., Poulter, B., Rehder, G., Reimer, J., Rodenbeck, C., Schwinger, J., Seferian, R., Skjelvan, I., Stocker, B. D., Tian, H. Q., Tilbrook, B., Tubiello, F. N., van der Laan-Luijkx, I. T., van der Werf, G. R., van Heuven, S., Viovy, N., Vuichard, N., Walker, A. P., Watson, A. J., Wiltshire, A. J., Zaehle, S., and Zhu, D.: Global Carbon Budget 2017, Earth Syst Sci Data, 10, 405-448, 10.5194/essd-10-405-2018, 2018.
Lohmann, U., and Feichter, J.: Global indirect aerosol effects: a review, Atmospheric Chemistry and Physics, 5, 715-737, 2005.
Mann, M. E., Miller, S. K., Rahmstorf, S., Steinman, B. A., and Tingley, M.: Record temperature streak bears anthropogenic fingerprint, Geophys Res Lett, 44, 7936-7944, 10.1002/2017gl074056, 2017.
Meinshausen, M., Smith, S. J., Calvin, K., Daniel, J. S., Kainuma, M. L. T., Lamarque, J. F.,

Matsumoto, K., Montzka, S. A., Raper, S. C. B., Riahi, K., Thomson, A., Velders, G. J. M., and van Vuuren, D. P. P.: The RCP greenhouse gas concentrations and their extensions from 1765 to 2300, Climatic Change, 109, 213-241, 10.1007/S10584-011-0156-Z, 2011.

Mengis, N., Partanen, A.-I., Jalbert, J., and Matthews, H. D.: 1.5 °C carbon budget dependent on carbon cycle uncertainty and future non-CO2 forcing, Scientific Reports, 8, 5831, 2018.

Mercado, L. M., Bellouin, N., Sitch, S., Boucher, O., Huntingford, C., Wild, M., and Cox, P. M.: Impact of changes in diffuse radiation on the global land carbon sink, Nature, 458, 1014-U1087, 10.1038/Nature07949, 2009.

Millar, R. J., Fuglestvedt, J. S., Friedlingstein, P., Rogelj, J., Grubb, M. J., Matthews, H. D., Skeie, R. B., Forster, P. M., Frame, D. J., and Allen, A. R.: Emission budgets and pathways consistent with limiting warming to 1.5 degrees C, Nat Geosci, 10, 741-747, 10.1038/Ngeo3031, 2017.

Mitchell, D., Heaviside, C., Schaller, N., Allen, M., Ebi, K. L., Fischer, E. M., Gasparrini, A., Harrington, L., Kharin, V., Shiogama, H., Sillmann, J., Sippel, S., and Vardoulakis, S.: Extreme heat-related mortality avoided under Paris Agreement goals, Nat Clim Change, 8, 551-553, 10.1038/s41558-018-0210-1, 2018.

Mu, Q. Z., Zhao, M. S., Running, S. W., Liu, M. L., and Tian, H. Q.: Contribution of increasing CO(2) and climate change to the carbon cycle in China's ecosystems, J Geophys Res-Biogeo, 113, G01018, 10.1029/2006jg000316, 2008.

Nangombe, S., Zhou, T., Zhang, W., Wu, B., Hu, S., Zou, L., and Li, D.: Record-breaking climate extremes in Africa under stabilized 1.5°C and 2°C global warming scenarios, Nat Clim Change, 8, 375-380, 10.1038/s41558-018-0145-6, 2018.

Piao, S. L., Fang, J. Y., Ciais, P., Peylin, P., Huang, Y., Sitch, S., and Wang, T.: The carbon balance of terrestrial ecosystems in China, Nature, 458, 1009-U1082, 10.1038/nature07944, 2009.

Piao, S. L., Sitch, S., Ciais, P., Friedlingstein, P., Peylin, P., Wang, X. H., Ahlstrom, A., Anav, A., Canadell, J. G., Cong, N., Huntingford, C., Jung, M., Levis, S., Levy, P. E., Li, J. S., Lin, X., Lomas, M. R., Lu, M., Luo, Y. Q., Ma, Y. C., Myneni, R. B., Poulter, B., Sun, Z. Z., Wang, T., Viovy, N., Zaehle, S., and Zeng, N.: Evaluation of terrestrial carbon cycle models for their response to climate variability and to CO2 trends, Global Change Biol, 19, 2117-2132, 10.1111/Gcb.12187, 2013.

Rienecker, M. M., Suarez, M. J., Gelaro, R., Todling, R., Bacmeister, J., Liu, E., Bosilovich, M. G., Schubert, S. D., Takacs, L., Kim, G. K., Bloom, S., Chen, J. Y., Collins, D., Conaty, A., Da Silva, A., Gu, W., Joiner, J., Koster, R. D., Lucchesi, R., Molod, A., Owens, T., Pawson, S., Pegion, P., Redder, C. R., Reichle, R., Robertson, F. R., Ruddick, A. G., Sienkiewicz, M., and Woollen, J.: MERRA: NASA's Modern-Era Retrospective Analysis for Research and Applications, J Climate, 24, 3624-3648, 10.1175/Jcli-D-11-00015.1, 2011.

Schaefer, K., Collatz, G. J., Tans, P., Denning, A. S., Baker, I., Berry, J., Prihodko, L., Suits, N., and Philpott, A.: Combined Simple Biosphere/Carnegie-Ames-Stanford Approach terrestrial carbon cycle model, J. Geophys. Res., 113, G03034, 10.1029/2007jg000603, 2008.

Schmidt, G. A., Kelley, M., Nazarenko, L., Ruedy, R., Russell, G. L., Aleinov, I., Bauer, M., Bauer, S. E., Bhat, M. K., Bleck, R., Canuto, V., Chen, Y. H., Cheng, Y., Clune, T. L., Del Genio, A., de Fainchtein, R., Faluvegi, G., Hansen, J. E., Healy, R. J., Kiang, N. Y., Koch, D., Lacis, A. A., LeGrande, A. N., Lerner, J., Lo, K. K., Matthews, E. E., Menon, S., Miller, R. L., Oinas, V., Oloso, A. O., Perlwitz, J. P., Puma, M. J., Putman, W. M., Rind, D., Romanou, A., Sato, M., Shindell, D. T., Sun, S., Syed, R. A., Tausnev, N., Tsigaridis, K., Unger, N., Voulgarakis, A.,

Yao, M. S., and Zhang, J. L.: Configuration and assessment of the GISS ModelE2 contributions to the CMIP5 archive, J Adv Model Earth Sy, 6, 141-184, 10.1002/2013ms000265, 2014.

Sitch, S., Cox, P. M., Collins, W. J., and Huntingford, C.: Indirect radiative forcing of climate change through ozone effects on the land-carbon sink, Nature, 448, 791-794, 10.1038/Nature06059, 2007.

Smith, W. K., Reed, S. C., Cleveland, C. C., Ballantyne, A. P., Anderegg, W. R. L., Wieder, W. R., Liu, Y. Y., and Running, S. W.: Large divergence of satellite and Earth system model estimates of global terrestrial CO2 fertilization, Nat Clim Change, 6, 306-310, 10.1038/Nclimate2879, 2016.

Solomon, S., Plattner, G.-K., Knutti, R., and Friedlingstein, P.: Irreversible climate change due to carbon dioxide emissions, P Natl Acad Sci USA, 106, 1704-1709, 10.1073/pnas.0812721106, 2009.

Spitters, C. J. T.: Separating the Diffuse and Direct Component of Global Radiation and Its Implications for Modeling Canopy Photosynthesis .2. Calculation of Canopy Photosynthesis, Agr Forest Meteorol, 38, 231-242, 10.1016/0168-1923(86)90061-4, 1986.

Stehfest, E., Zeist, W.-J. v., Valin, H., Havlik, P., Popp, A., Kyle, P., Tabeau, A., Mason-D'Croz, D., Hasegawa, T., Bodirsky, B. L., Calvin, K., Doelman, J. C., Fujimori, S., Humpenöder, F., Lotze-Campen, H., Meijl, H. v., and Wiebe, K.: Key determinants of global land-use projections, Nat Commun, 10, 2166, 2019.

Tian, H. Q., Xu, X. F., Lu, C. Q., Liu, M. L., Ren, W., Chen, G. S., Melillo, J., and Liu, J. Y.: Net exchanges of CO2, CH4, and N2O between China's terrestrial ecosystems and the atmosphere and their contributions to global climate warming, Journal of Geophysical Research, 116, G02011, 10.1029/2010jg001393, 2011.

Warszawski, L., Friend, A., Ostberg, S., Frieler, K., Lucht, W., Schaphoff, S., Beerling, D., Cadule, P., Ciais, P., Clark, D. B., Kahana, R., Ito, A., Keribin, R., Kleidon, A., Lomas, M., Nishina, K., Pavlick, R., Rademacher, T. T., Buechner, M., Piontek, F., Schewe, J., Serdeczny, O., and Schellnhuber, H. J.: A multi-model analysis of risk of ecosystem shifts under climate change, Environ Res Lett, 8, 044018, 10.1088/1748-9326/8/4/044018, 2013.

Weedon, G. P., Balsamo, G., Bellouin, N., Gomes, S., Best, M. J., and Viterbo, P.: The WFDEI meteorological forcing data set: WATCH Forcing Data methodology applied to ERA-Interim reanalysis data, Water Resources Research, 50, 7505-7514, 10.1002/2014wr015638, 2014.

Wu, S., Yin, Y., Zhao, D., Huang, M., Shao, X., and Dai, E.: Impact of future climate change on terrestrial ecosystems in China, International Journal of Climatology, 30, 866-873, 10.1002/joc.1938, 2009.

Xiao, J. F., Zhou, Y., and Zhang, L.: Contributions of natural and human factors to increases in vegetation productivity in China, Ecosphere, 6, 233, 10.1890/Es14-00394.1, 2015.

Yao, Y. T., Wang, X. H., Li, Y., Wang, T., Shen, M. G., Du, M. Y., He, H. L., Li, Y. N., Luo, W. J., Ma, M. G., Ma, Y. M., Tang, Y. H., Wang, H. M., Zhang, X. Z., Zhang, Y. P., Zhao, L., Zhou, G. S., and Piao, S. L.: Spatiotemporal pattern of gross primary productivity and its covariation with climate in China over the last thirty years, Global Change Biol, 24, 184-196, 10.1111/gcb.13830, 2018.

Yu, H., Kaufman, Y. J., Chin, M., Feingold, G., Remer, L. A., Anderson, T. L., Balkanski, Y., Bellouin, N., Boucher, O., Christopher, S., DeCola, P., Kahn, R., Koch, D., Loeb, N., Reddy, M. S., Schulz, M., Takemura, T., and Zhou, M.: A review of measurement-based assessments

Formatted: Font:10.5 pt

of the aerosol direct radiative effect and forcing, Atmos. Chem. Phys., 6, 613-666, 2006.

Yue, X., and Unger, N.: The Yale Interactive terrestrial Biosphere model: description, evaluation and implementation into NASA GISS ModelE2, Geosci Model Dev, 8, 2399-2417, 10.5194/gmd-8-2399-2015, 2015.

Yue, X., and Unger, N.: Aerosol optical depth thresholds as a tool to assess diffuse radiation fertilization of the land carbon uptake in China, Atmospheric Chemistry and Physics, 17, 1329-1342, 10.5194/acp-17-1329-2017, 2017.

Yue, X., Unger, N., Harper, K., Xia, X., Liao, H., Zhu, T., Xiao, J., Feng, Z., and Li, J.: Ozone and haze pollution weakens net primary productivity in China, Atmospheric Chemistry and Physics, 17, 6073-6089, 10.5194/acp-17-6073-2017, 2017.

Yue, X., and Unger, N.: Fire air pollution reduces global terrestrial productivity, Nat Commun, 9, 5413, 10.1038/s41467-018-07921-4, 2018.

Zaehle, S., Medlyn, B. E., De Kauwe, M. G., Walker, A. P., Dietze, M. C., Hickler, T., Luo, Y. Q., Wang, Y. P., El-Masri, B., Thornton, P., Jain, A., Wang, S. S., Warlind, D., Weng, E. S., Parton, W., Iversen, C. M., Gallet-Budynek, A., McCarthy, H., Finzi, A. C., Hanson, P. J., Prentice, I. C., Oren, R., and Norby, R. J.: Evaluation of 11 terrestrial carbon-nitrogen cycle models against observations from two temperate Free-Air CO2 Enrichment studies, New Phytol, 202, 803-822, 10.1111/Nph.12697, 2014.

Formatted: Font:10.5 pt

Formatted: Font:Times New Roman, 10.5 pt

Author Contributions

X.Y., H.L., and H.W. designed the research and wrote the manuscript. X.Y. downloaded CMIP5 data, set up models, and performed all simulations. T.Z. evaluated diffuse radiation models. N.U. provided ACCMIP data. S.S. provided TRENDY data. Z.F. provided O_3 damaging meta-analysis data in China. J.Y. analyzed TRENDY results over China. All authors contributed to the interpretation of the results and improvement of the paper.

Acknowledgements

This work is supported by the National Key Research and Development Program of China (grant no. 2017YFA0603802) and National Natural Science Foundation of China (grant no. 91744311).

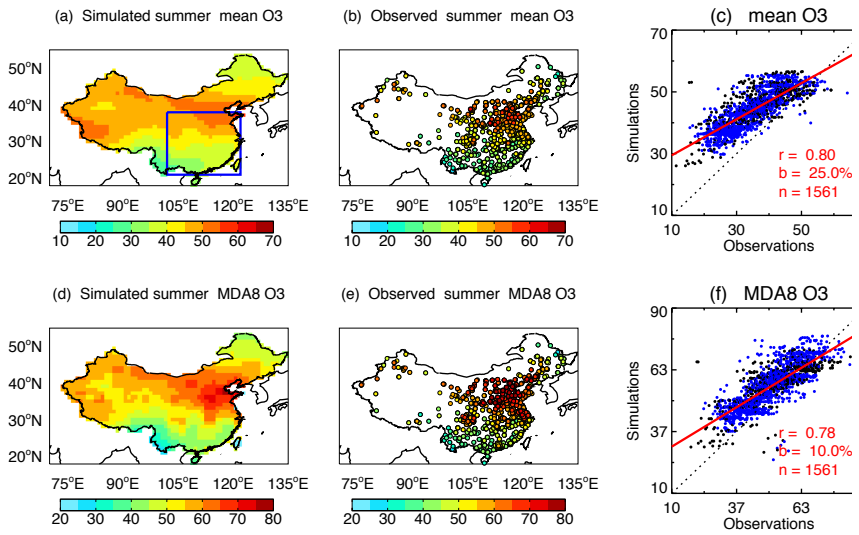

Figure 1. Evaluation of surface O_3 with site-level observations. Simulations are ensemble (a) mean and (d) daily maximum 8-hour average (MDA8) O_3 for the period of 2005-2015 from 12 ACCMIP models. Observations (b and e) are the average during 2015-2018 from 1580 sites operated by Ministry of Ecology and Environment, China. The correlation coefficients (r), relative biases (b), and number of sites (n, excluding data-missing sites) are shown in the scatter plots (c and f). The blue points in the scatter plots represent sites located within the box regions in eastern China as shown in (a). The dashed line represents the 1:1 ratio. The red line is the linear regression between simulations and observations.

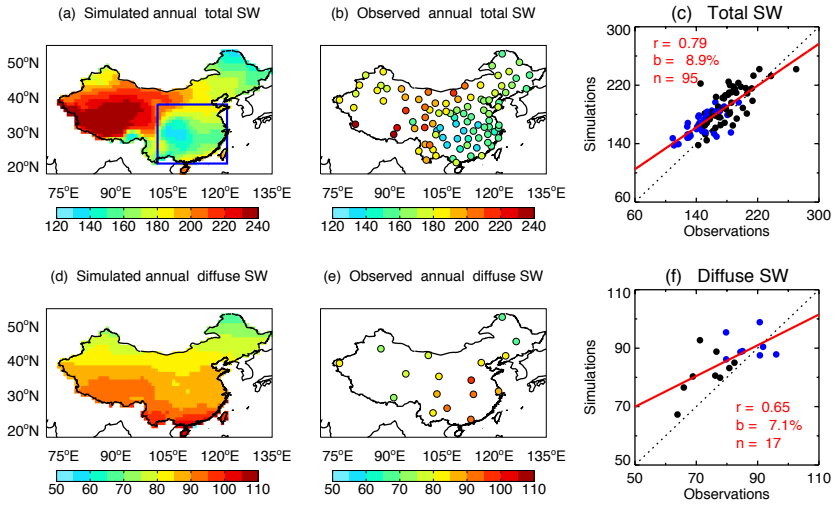

772

773 **Figure 2**. Evaluation of radiation fluxes with site-level observations. Simulations are surface (a)
774 total shortwave radiation (W m^{-2}) and (d) diffuse radiation derived with method M01 (Table S4) for
775 the period of 2005-2015 from an ensemble of 7 CMIP5 climate models. Observations (b and e) are
776 the average during 2009-2011 from 106 sites operated by the Climate Data Center, Chinese
777 Meteorological Administration. The correlation coefficients (r), relative biases (b), and number of
778 sites (n, excluding data-missing sites) are shown in the scatter plots (c and f). The blue points in the
779 scatter plots represent sites located within the box regions in eastern China as shown in (a). The
780 dashed line represents the 1:1 ratio. The red line is the linear regression between simulations and
781 observations.

782

783

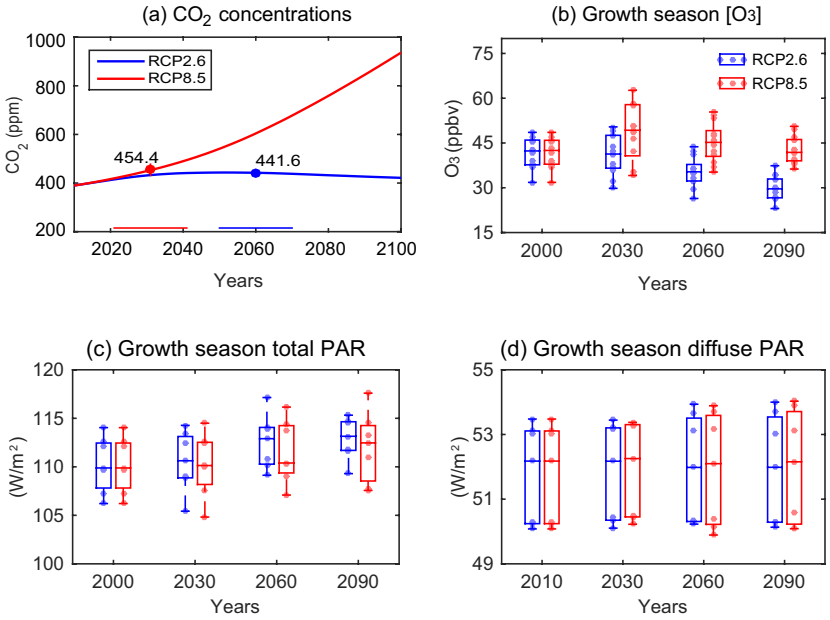

Figure 3. Changes in atmospheric compositions and radiation. Results shown are projected future (a) global CO_2 concentrations, and (b) surface O_3 concentrations, (c) total Photosynthetically Active Radiation (PAR), and (d) diffuse PAR at growth season in China. The average (a) CO_2 concentrations at the global warming of 1.5°C are 442 ppm for RCP2.6 scenario (blue, 2050-2070) and 454 ppm for RCP8.5 scenario (red, 2021-2041). The (b) O_3 concentrations are averaged over east of 110ºE in China from 12 ACCMIP models for RCP2.6 (blue) and RCP8.5 (red) scenarios. Each dot represents the value averaged for May to September from a chemistry model. The (c-d) PAR values are averaged over China from 7 CMIP5 models for RCP2.6 (blue) and RCP8.5 (red) scenarios. Diffuse PAR is calculated using hourly total PAR and solar zenith angle based on the parameterization M01. Each dot represents the value averaged for May to September from a climate model. For each selected year in (b-d), a period of 11 years (5 years before and 5 years after) is used to derive the decadal mean values.

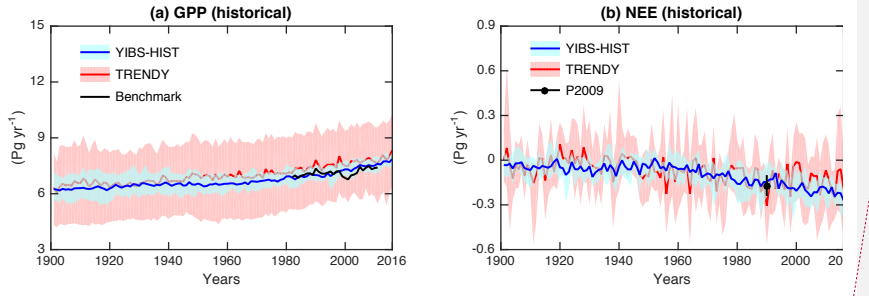

Deleted:

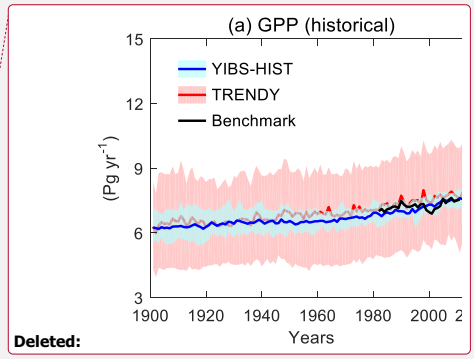

Figure 4. Historical carbon fluxes in China. Results shown are simulated (a) gross primary productivity (GPP) and (b) net ecosystem exchange (NEE) during historical period (1901-2016) using YIBs model (blue), and the comparison with predictions of 14 terrestrial models from TRENDY project (red). The bold lines are ensemble means with red shadings for inter-vegetation-model uncertainties and blue shadings for inter-climate-model uncertainties. All YIBs simulations are driven with daily meteorology from CMIP5 models. All TRENDY simulations are driven with CRUNCEP meteorology. The black line in (a) represents benchmark results of 1980-2011 from Jung et al. (2009). The black point with error bar in (b) represents the synthesis of ground- and model-based estimate of NEE in China by Piao et al. (2009).

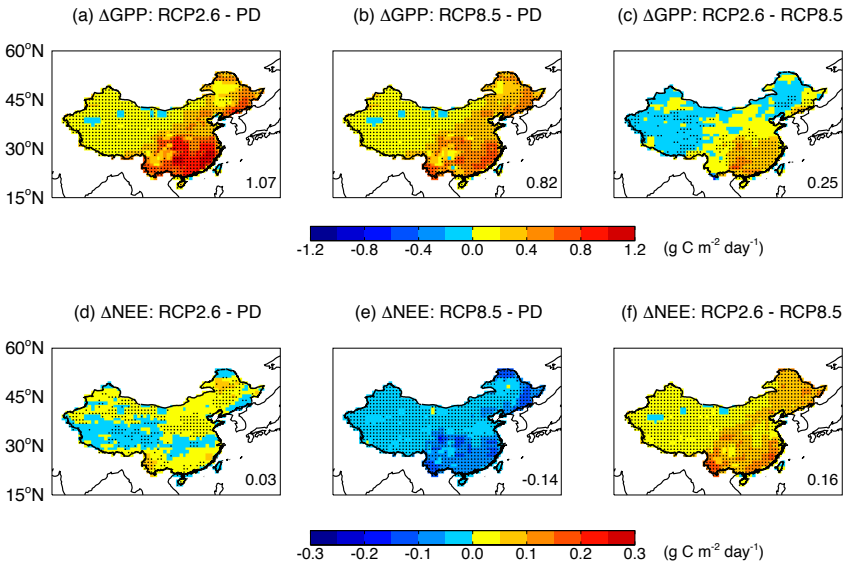

Figure 5. Changes in carbon fluxes by global warming of 1.5ºC. Results shown are simulated (top) GPP and (bottom) NEE over China between the period of global warming of 1.5ºC and present day (1995-2015) under (left) RCP2.6 scenario, (middle) RCP8.5 scenario, and (right) their differences. The period of global warming of 1.5 ºC is set to 2050-2070 for RCP2.6 and 2021-2041 for RCP8.5. Simulations are performed using YIBs vegetation model driven with daily meteorology from 7 CMIP5 models. The O_3 damaging effect is included with predicted ensemble O_3 concentrations from 12 ACCMIP models. For each grid, significant changes at $p<0.05$ are marked with dots. The total changes (Pg C yr^{-1}) over China are shown in each panel.

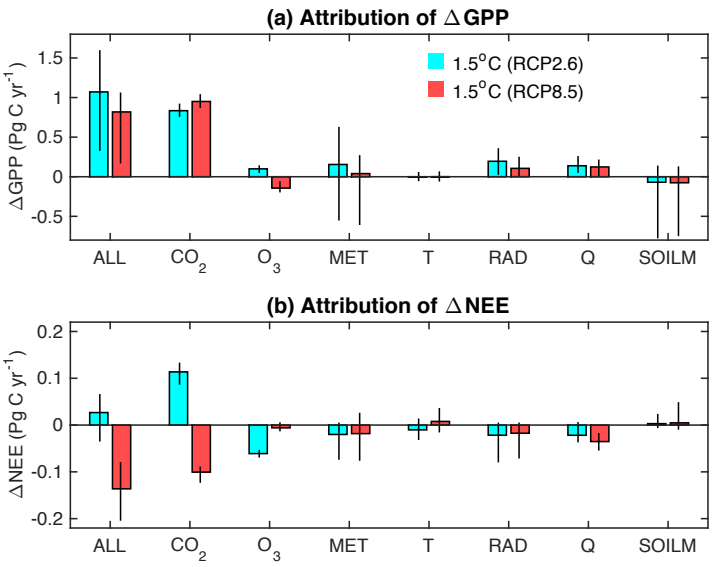

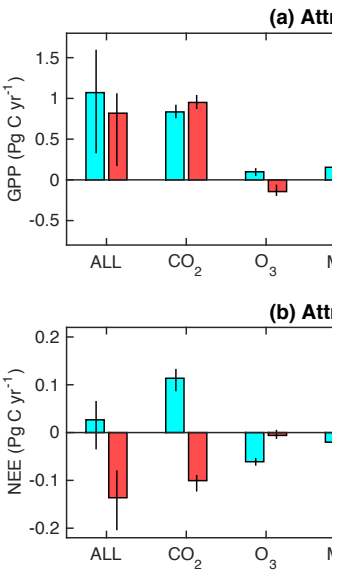

Deleted:

Figure 6. Attribution of changes in GPP and NEE to individual driving factors. Results shown are the predicted GPP changes in China between the period of global warming of 1.5ºC and present day (1995-2015) caused by all (ALL) or individual driving factors, including CO_2 fertilization, O_3 damaging, and meteorological changes (MET). The perturbations by meteorology is a combination of those by temperature (T), radiation (RAD), specific humidity (Q), and soil moisture (SOILM). The contrast is shown between the scenarios of RCP2.6 (blue, 2050-2070) and RCP8.5 (red, 2021-2041). The error bars indicate uncertainties of YIBs simulations using different future meteorology from 7 CMIP5 models.

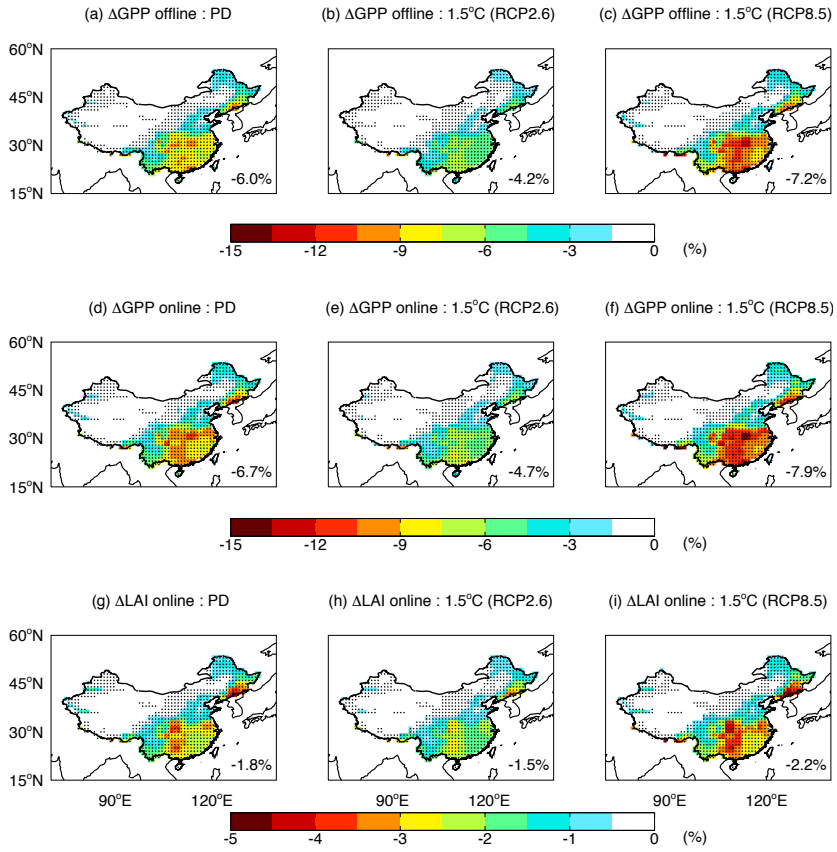

Figure 7. Damaging effects of O_3 to photosynthesis and plant growth. Results shown are ensemble mean changes in (top) offline GPP, (middle) online GPP, and (bottom) leaf area index (LAI) caused by O_3 at (left) present day (1995-2015) and 1.5°C warming under (middle) RCP.6 (2050-2070) and (right) RCP8.5 (2021-2041) scenarios. The simulations are performed with YIBs vegetation model driven with meteorology from 7 CMIP5 models and hourly ozone derived from 12 ACCMIP models. The damaging effect is averaged for high and low O_3 sensitivities. For each grid, significant changes at $p<0.05$ are marked with dots. The mean changes over China are shown in each panel.

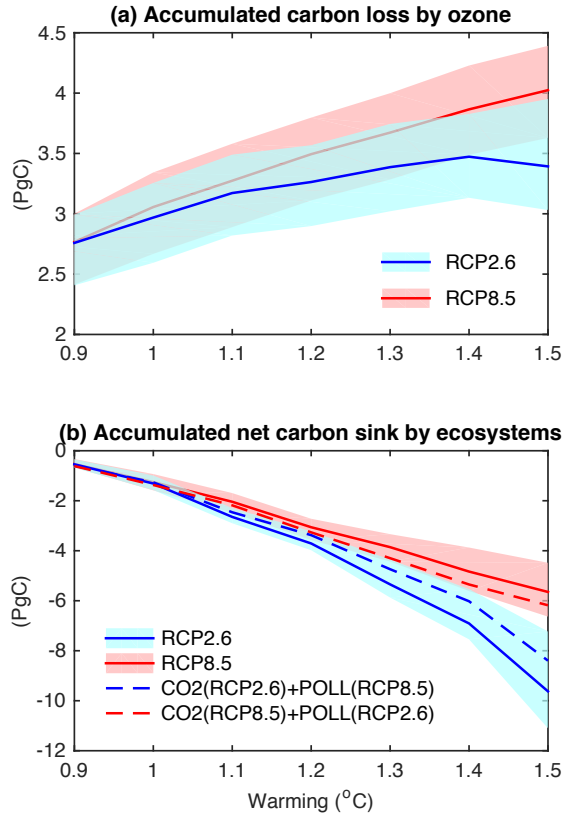

Figure 8. Accumulated carbon budget in China by 1.5ºC global warming. The top panel shows the total carbon loss of ecosystems caused by O_3 damaging effects at different warming thresholds for two emission pathways. The bottom panel shows the accumulated net carbon sink by ecosystems in China at the 1.5ºC global warming. The two solid lines represent emissions of CO_2 and pollutants from the same scenario, either RCP2.6 (blue) or RCP8.5 (red). The dashed lines represent sensitivity experiments with inconsistent CO_2 and pollutants, with the blue (red) line driven with CO_2 from RCP2.6 (RCP8.5) but air pollution from RCP8.5 (RCP2.6). The warming of 1.0 ºC is the year 2010 for both RCP2.6 and RCP8.5 scenarios.

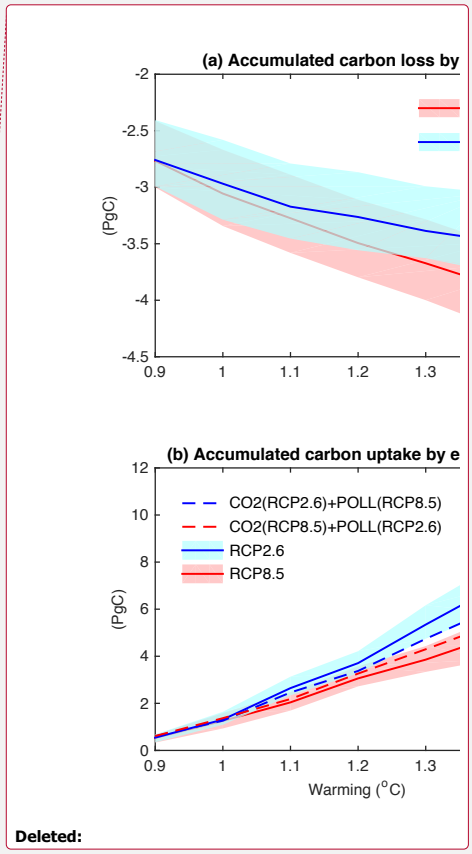

Deleted:

Deleted: total

Deleted: uptake